Inversion-free stabilization and regulation of systems with hysteresis via integral action[☆]

Alex Esbrook [1], Xiaobo Tan, Hassan K. Khalil

Department of Electrical and Computer Engineering, Michigan State University, East Lansing, MI 48824, USA

ARTICLE INFO

ABSTRACT

In this paper, we present conditions for the stabilization and regulation of the tracking error for an n-dimensional minimum-phase system preceded by a Prandtl–Ishlinskii hysteresis operator. A general controller structure is considered; however, we assume that an integral action is present. The common Lyapunov function theorem is utilized together with a Linear Matrix Inequality (LMI) condition to show that, under suitable conditions, the tracking error of the system goes to zero exponentially fast when a constant reference is considered. A key feature of this LMI condition is that it does not require the hysteresis effect to be small, meaning that hysteresis inversion is not required. We use this condition together with a periodicity assumption to prove that a servocompensator-based controller can stabilize the system without using hysteresis inversion. Additionally, we draw parallels between our LMI condition and passivity-based results achieved in the literature. We then verify our LMI results in simulation, where we show that the LMI condition can accurately predict the stability margins of a system with hysteresis. Finally, we conduct experiments using a servocompensator-based controller, where we verify the stability of the system and achieve a mean tracking error of 0.5% for a 200 Hz sinusoidal reference.

© 2013 Elsevier Ltd. All rights reserved.

1. Introduction

Smart materials have become a popular topic of research in the field of engineering, due to a number of emerging applications employing these novel materials (Eaton et al., 2007). The control of smart materials is a complicated and interesting topic, due in great deal to the phenomenon of hysteresis, which smart materials ubiquitously exhibit. The theory of mathematical models of hysteresis, known as hysteresis operators (Brokate & Sprekels, 1996; Mayergoyz, 1991), were formalized in the 1970s. Examples of such models include the Preisach operator (Tan & Baras, 2005), Prandtl–Ishlinskii (PI) operator (Janaideh, Rakheja, & Su, 2009), and the Preisach–Krasnosel'skii–Pokrovskii (PKP) operator (Webb, Lagoudas, & Kurdila, 1998). Each of these operators is based on the weighted superposition of many (and even infinitely many) elementary hysteretic units called hysterons. Other examples of hysteresis operators include the Duhem model (Oh & Bernstein, 2005; Visintin, 1994) and Bouc–Wen model (Ikhouane & Rodellar, 2007). These hysteresis operators form the basis of many smart material models.

While a number of models for smart materials exist, a common model structure for smart material actuators is a linear dynamical system preceded by a hysteresis operator (Chen, Tan, & Shahinpoor, 2005; Davino, Natale, Pirozzi, & Visone, 2004; Janaideh et al., 2009). Such models are especially common in the field of nanopositioning, where piezoelectric actuators are used to generate controllable motion with nanometer resolution. A wide variety of control techniques have been proposed for such systems (Devasia, Eleftheriou, & Moheimani, 2007), including sliding-mode control (Bashash & Jalili, 2009), adaptive control (Tao & Kokotovic, 1995), two-degree-of-freedom control (Lee & Salapaka, 2009), and many more (Wu & Zou, 2007; Zhong & Yao, 2008). In particular, hysteresis inversion (Ahrens, Tan, & Khalil, 2009; Cavallo, Natale, Pirozzi, & Visone, 2003; Ge & Jouaneh, 1996; Iyer & Tan, 2009) has been used extensively due to its effectiveness in mitigating the effect of hysteresis on the system.

Many of the above mentioned results have focused on proving boundedness of states by considering hysteresis as a disturbance. A new wave of research over the past five years has focused on direct analysis of systems with hysteresis, based on the mathematical formulations of the hysteresis operators. These works have provided some analytical results showing the stability of systems with hysteresis and convergence of the tracking error to zero, and

importantly, can do so without hysteresis inversion or requiring the hysteresis effect to be small. Such a result was proved in Riccardi, Naso, Turchiano, Janocha, and Palagachev (2012), where an LMI framework is utilized to provide sufficient conditions for the stability and tracking error convergence for a PID-controlled linear system without zero dynamics preceded by a modified PI operator (Kuhnen, 2003). In Valadkhan, Morris, and Khajepour (2010), stability and tracking error convergence of a non-dynamic plant modeled by a Preisach operator was proved using monotonic properties of the operator. The authors of Jayawardhana, Logemann, and Ryan (2008) proved closed-loop stability for a system involving a PID-controlled second-order system preceded by a general hysteresis operator, and provided guidelines on the selection of controller gains. The circle criterion was also utilized to prove stability of systems with hysteresis in Jayawardhana, Logemann, and Ryan (2011).

One weakness of these results is that many are proved for dynamic systems of second order or lower. Similar results for nth-order systems have typically relied on passivity conditions. One of the most well known results in this area is reported in Gorbet, Morris, and Wang (2001), where a Preisach operator is shown to be dissipative. This is then combined with traditional passivity results to show the finite-gain stability of the system. Dissipative properties have also been shown for the PI operator (Brokate & Sprekels, 1996) and the Duhem operator (Jayawardhana & Andrieu, 2009). A shortcoming of these results is that they are able to only show boundedness, even for constant reference trajectories. In addition, the conditions required for passivity are not satisfied by many plants and controllers. Outside of passivity focused results, an interesting contribution is from Barreiro and Banos (2005), where tight input–output stability bounds are shown for systems with play operators without explicit passivity assumptions. Finally, in Tarbouriech, Prieur, and Queinnec (2010), stability of an n-dimensional system is proved under an LMI condition; however, this result did not consider any controller, and furthermore, did not show that tracking error could be regulated.

In this paper, we discuss the stability and tracking error convergence of a system with hysteresis using a general feedback controller containing an integral action. It is assumed that the hysteresis is modeled by a Prandtl–Ishlinskii (PI) operator, which has become a popular model for smart material hysteresis (Croft, Shed, & Devasia, 2001; Devasia et al., 2007; Wu & Zou, 2007). The theory of switched systems, in particular, that of the common Lyapunov function (Decarlo, Branicky, Pettersson, & Lennartson, 2000), and a linear matrix inequality (LMI) condition will be used to prove that the tracking error and state vector converge exponentially to zero for a constant reference. The principal contribution of this work is to present sufficient conditions (in the form of an LMI) for the regulation of the closed-loop system in terms of the hysteresis parameters, without requiring the hysteresis to be small. This condition can be utilized in an iterative design procedure in order to stabilize a system with hysteresis modeled by a PI operator. As we will see, the presence of an integral action is crucial to the formulation of our LMI condition. Comparing our LMI results to those achieved in Riccardi et al. (2012) and Tarbouriech et al. (2010), the proposed framework can handle minimum-phase systems of arbitrary order, in contrast to Riccardi et al. (2012), as well as a wide class of controllers, in contrast to both (Riccardi et al., 2012) and (Tarbouriech et al., 2010). The class of controllers which can be incorporated into this design framework includes Servocompensators, which have shown great promise in the control of systems with hysteresis, particularly nanopositioning systems (Esbrook, Tan, & Khalil, in preparation).

We then connect our LMI result to the aforementioned passivity results, by demonstrating that if the system obeys a certain positive real condition, a solution to the LMI problem can be found analytically. In addition, we apply our LMI results to show that servocompensator-based controllers can stabilize systems with
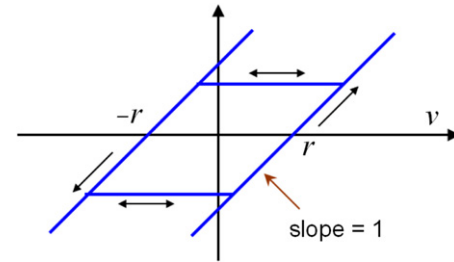

Fig. 1. Illustration of a play operator.

hysteresis, without requiring inversion of the hysteresis. Our simulation results then confirm the effectiveness of the LMI condition at predicting the global convergence of the tracking error.

We then verify our results through experiments conducted on a commercial nanopositioner. These experiments focused on comparing the performance of servocompensator-based controllers (Esbrook et al., in preparation) with and without hysteresis inversion. We first verify the LMI condition presented in the paper, in order to prove stability of the system. Our experimental results indicate that servocompensator-based controllers without hysteresis inversion can achieve half the mean tracking error as that achieved by the same control method with inversion, while also being less computationally intensive.

The remainder of this paper is organized as follows. Section 2 introduces the PI hysteresis operator used in this work. Section 3 contains the main results of the paper, showing tracking error convergence and exponential stability for the closed-loop system. This result is then extended in Section 4 where we provide specialized results for cases of servocompensator-based controllers. Simulation results confirming our LMI results are presented in Section 5. Section 6 contains the experimental results of the paper, and concluding remarks are presented in Section 7.

2. The Prandtl–Ishlinskii operator

In this section, we provide a review of the Prandtl–Ishlinskii (PI) hysteresis operator (Brokate & Sprekels, 1996; Kuhnen, 2003). The PI operator consists of a weighted superposition of basic hysteretic units called play operators, shown in Fig. 1. Each play operator P_r is parameterized by a parameter r, representing the play radius or threshold. When the input $v(t)$ is monotone and continuous, we can express the output $u_r(t)$ of a play operator P_r as

$$u_r(t) = P_r[v; u_r(0)](t)$$
$$= \max(\min(v(t) + r, u_r(0)), v(t) - r). \quad (1)$$

The output $u_r(t)$ is also referred to as the state of the play operator P_r. For general inputs, the input signal is broken into monotone segments, and the output is then calculated by setting the last output of one monotone segment as the initial condition for the next. Notice from Fig. 1 and (1) that there are two basic modes in which the state of a play operator can reside. The first is the linear region, in which $u_r(t) = v(t) \pm r$. The second mode of operation is the play region, where $u_r(t)$ is constant, represented in (1) by the term $u_r(0)$. We will make use of the linear and play region terminology throughout the paper.

In general, the PI operator is an infinite-dimensional operator, comprised of a continuum of play operators integrated over some interval of play radii. However, in the interest of practical implementation, we will consider only a finite-dimensional PI operator, representable by a weighted sum of a finite number of play operators. The output of the PI operator Γ_h under an input v is then given by

$$u(t) = \Gamma_h[v; W(0)](t) = \sum_{i=0}^{o} \theta_i P_{r_i}[v; W_i(0)](t) \quad (2)$$

$W_i(t)$ represents the state of the play operator P_{r_i} at time t, and

$$W(t) \triangleq [W_0(t), W_1(t), \ldots, W_o(t)]^T$$

where the superscript ^{T} denotes the transpose, and $W(0)$ represents the initial condition of the operator Γ_h. The vector $\theta = [\theta_0, \theta_1, \ldots, \theta_o]^T$ represents the weights of individual play elements of the operator, where each θ_i is assumed to be bounded and nonnegative. We will use $\mathbf{r}$ to denote the vector of radii, $\mathbf{r} = [r_0, r_1, \ldots, r_o]^T$, where $r_0 = 0$. We also define the operator $\mathcal{P} \triangleq [P_{r_0}, P_{r_1}, \ldots, P_{r_o}]^T$, which captures the evolution of the state $W(t)$ of Γ_h under input v, i.e.,

$$W(t) = \mathcal{P}[v; W(0)](t). \tag{3}$$

This will allow us to write the output $u(t)$ as

$$u(t) = \theta^T W(t). \tag{4}$$

It is conventional to include the $r_0 = 0$ term in the definition of the hysteresis operator, even though this term results in simply a linear gain. For our work, we will separate this term from the nonzero radii play operators, thus

$$u(t) = \theta_0 v(t) + \theta_h^T W_h(t) \tag{5}$$

where

$$\theta_h = [\theta_1, \ldots, \theta_o]^T,$$
$$\mathcal{P}_h \triangleq [P_{r_1}, \ldots, P_{r_o}]^T,$$
$$W_h(t) = \mathcal{P}_h[v; W_h(0)](t).$$

3. Sufficient conditions for stability in systems with hysteresis

Having presented our hysteresis model, we are now prepared to discuss the stabilization problem for systems with hysteresis. Consider an n-dimensional linear system with transfer function,

$$\mathbb{G}_p(s) = \frac{k(s^m + b_{m-1}s^{m-1} + \cdots + b_1 s + b_0)}{s^n + a_{n-1}s^{n-1} + \cdots + a_1 s + a_0}, \quad m < n \tag{6}$$

with input $u(t)$ and output $y(t)$. We will assume that this transfer function is minimum phase. Our control objective is to regulate the output of the cascade connection of a PI operator (4) and $\mathbb{G}_p(s)$, illustrated in Fig. 2. In particular, we will design the input $v(t)$ to the hysteresis to stabilize the resulting feedback connection, and also drive y to a constant reference y_r. We will consider a normal-form state-space representation for the transfer function $\mathbb{G}_p(s)$ (Khalil, 2002),

$$\dot{z}(t) = Fz(t) + Gx_1(t) \tag{7}$$
$$\dot{x}(t) = A_0 x(t) + B(u(t) + \lambda x(t) + \psi z(t)) \tag{8}$$
$$y(t) = Cx = x_1(t) \tag{9}$$

where $u(t)$ obeys (5). The matrices $F \in \Re^{m \times m}$, $G \in \Re^m$, $A_0 \in \Re^{p \times p}$, and $B \in \Re^p$ are given by

$$F = \begin{bmatrix} 0 & 1 & \cdots & 0 \\ 0 & & \ddots & 0 \\ 0 & \cdots & \cdots & 1 \\ -b_0 & -b_1 & \cdots & -b_{m-1} \end{bmatrix}, \quad G = \begin{bmatrix} 0 \\ \vdots \\ 1 \end{bmatrix},$$

$$A_0 = \begin{bmatrix} 0 & 1 & \cdots & 0 \\ 0 & & \ddots & 0 \\ 0 & \cdots & \cdots & 1 \\ 0 & \cdots & 0 & 0 \end{bmatrix}, \quad B = \begin{bmatrix} 0 \\ \vdots \\ k \end{bmatrix},$$

and $\lambda \in \Re^{1 \times p}$, $\psi \in \Re^{1 \times m}$ are row vectors.

Remark 1. For simplicity but without loss of generality, we will assume in the following equations that $\theta_0 = 1$. This is because the gain of the hysteresis operator can be rolled into the DC gain of the linear dynamics. In order to transform a system where $\theta_0 \neq 1$ into
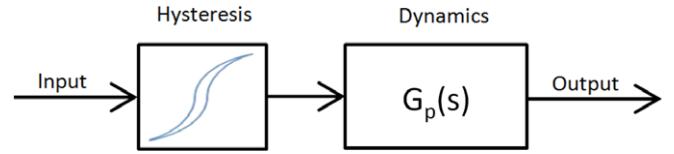

Fig. 2. Illustration of linear plant preceded by hysteresis operator, commonly used to model piezoelectric-actuated nanopositioners.

the form considered here, we multiply k in B by θ_0, and divide the elements of θ_h, λ, and ψ by the same value.

We will consider a general linear controller to control (5), (7)–(9). The controller includes a dynamic compensator represented in the state-space form,

$$\dot{\eta}(t) = C^* \eta(t) + B^*(x_1 - y_r) \tag{10}$$

with $C^* \in \Re^{q \times q}$ and $B^* \in \Re^q$. Here we use the tracking error $x_1 - y_r$ as an input to the controller; however, our analysis could be adjusted to accommodate different inputs. We will also require our linear controller to contain an integral action,

$$\dot{\sigma}(t) = x_1 - y_r. \tag{11}$$

Using (10) and (11), we can define our control signal to the plant/hysteresis operator;

$$v(t) = -K_1 z(t) - K_2 x(t) - K_3 \eta(t) - K_4 \sigma(t) \tag{12}$$

where $K_1 \in \Re^{1 \times m}$, $K_2 \in \Re^{1 \times p}$, $K_3 \in \Re^{1 \times q}$, and $K_4 \in \Re$ are constant gains. Applying (5) and (10)–(12) to (7)–(9) yields,

$$\begin{bmatrix} \dot{z}(t) \\ \dot{x}(t) \\ \dot{\eta}(t) \\ \dot{\sigma}(t) \end{bmatrix} = \begin{bmatrix} F & GC & 0 & 0 \\ -B(K_1 - \psi) & A_0 - B(K_2 - \lambda) & -BK_3 & -BK_4 \\ 0 & B^*C & C^* & 0 \\ 0 & C & 0 & 0 \end{bmatrix}$$
$$\cdot \begin{bmatrix} z(t) \\ x(t) \\ \eta(t) \\ \sigma(t) \end{bmatrix} + \begin{bmatrix} 0 \\ B\theta_h^T W_h[v; W_h(0)](t) \\ -B^* y_r \\ -y_r \end{bmatrix}. \tag{13}$$

As the PI operator is continuous, the system (12)–(13) is well-posed, and possesses a continuous and unique solution, which was proved in Tan and Khalil (2009). Next, define the coordinate transforms

$$\tilde{z}(t) = z(t) - [1, \mathbf{0}]^T \frac{1}{b_0} y_r \tag{14}$$

$$\tilde{x}(t) = x(t) - C^T y_r \tag{15}$$

where $\mathbf{0}$ is an $m - 1$ dimensional row vector of zeros. With these transforms, Eq. (13) then becomes

$$\begin{bmatrix} \dot{\tilde{z}}(t) \\ \dot{\tilde{x}}(t) \\ \dot{\eta}(t) \\ \dot{\sigma}(t) \end{bmatrix} = \begin{bmatrix} F & GC & 0 & 0 \\ -B(K_1 - \psi) & A_0 - B(K_2 - \lambda) & -BK_3 & -BK_4 \\ 0 & B^*C & C^* & 0 \\ 0 & C & 0 & 0 \end{bmatrix}$$
$$\cdot \begin{bmatrix} \tilde{z}(t) \\ \tilde{x}(t) \\ \eta(t) \\ \sigma(t) \end{bmatrix} + \begin{bmatrix} 0 \\ B\theta_h^T W_h[v; W_h(0)](t) + Bc_0 y_r \\ 0 \\ 0 \end{bmatrix} \tag{16}$$

where c_0 is a constant that depends on the system matrices and control gains, which appears due to the coordinate transform. We will now define

$$\alpha(t) = -K_4 \sigma(t) + \theta_h^T W_h[v; W_h(0)](t) + c_0 y_r. \tag{17}$$

This definition is made in order to use Lyapunov analysis to show that all states converge to the origin, since the state of the integrator will not necessarily go to zero in a system with hysteresis, even

if $y_r = 0$. The derivative of $\alpha(t)$ is given by

$$\dot{\alpha}(t) = -K_4 C \tilde{x}(t) + \theta_h^T \dot{W}_h[v; W_h(0)](t) \qquad (18)$$

where

$$\dot{W}_h[v; W_h(0)](t)$$
$$= [\dot{P}_{r_1}[v; W_1(0)](t), \ldots, \dot{P}_{r_m}[v; W_m(0)](t)]^T. \qquad (19)$$

The derivative of a play operator is in general discontinuous, as switching between play and linear regions can cause discontinuities in the value of $\dot{P}_{r_i}[v; W(0)](t)$. Let $\Pi(t)$ denote the set of all play operators $P_{r_i}[v; W(0)](t)$ that lie in a linear region at time t, and let Π^c denote its complement. We therefore have a piecewise expression for $\dot{P}_{r_i}$, given by

$$\dot{P}_{r_i}[v; W_i(0)](t) = \begin{cases} \dot{v}, & \text{if } i \in \Pi(t) \\ 0, & \text{if } i \in \Pi^c(t) \end{cases} \qquad (20)$$

where

$$\dot{v}(t) = -K_1[F\tilde{z}(t) + GC\tilde{x}(t)] - K_2[-B(K_1 - \psi)\tilde{z}(t)$$
$$+ (A_0 - B(K_2 - \lambda))\tilde{x}(t) - BK_3\eta(t) + B\alpha(t)]$$
$$- K_3[C^*\eta(t) + B^*C\tilde{x}(t)] - K_4[C\tilde{x}(t)]. \qquad (21)$$

Let Θ_h be the set of all numbers that can be reached by adding together elements of θ_h. Next, define $\bar{\theta}_h(t) \in \Theta_h$ as the summation of weights for play operators in the linear region, i.e.

$$\bar{\theta}_h(t) = \left[\sum_i \theta_{hi} : i \in \Pi(t) \right] \qquad (22)$$

Define the state vector

$$\gamma(t) = [\tilde{z}^T(t), \tilde{x}^T(t), \eta^T(t), \alpha(t)]^T.$$

Note that $\dot{v}$ can be expressed as a constant vector multiplying the state vector of the system, i.e. $\dot{v} = K_v \gamma$. Using this definition with (17) and (18), we transform (16) into

$$\dot{\gamma}(t) = \begin{bmatrix} F & GC & 0 & 0 \\ -B(K_1 - \psi) & A_0 - B(K_2 - \lambda) & -BK_3 & B \\ 0 & B^*C & C^* & 0 \\ 0 & -K_4C & 0 & 0 \end{bmatrix} \gamma(t)$$
$$+ \begin{bmatrix} 0 \\ 0 \\ 0 \\ \bar{\theta}_h(t)K_v\gamma(t) \end{bmatrix}. \qquad (23)$$

Note that by using α as our state variable, $c_0 y_r$ drops out of the analysis of the closed-loop system, as y_r is constant. Alternatively, we write (23) in a compact form,

$$\dot{\gamma}(t) \triangleq (\Sigma_0 + \bar{\theta}_h(t)\bar{B}K_v)\gamma(t) \qquad (24)$$

where

$$\bar{B} = [\mathbf{0}, 1]^T$$

where $\mathbf{0}$ here is an $m + p + q$ dimensional row vector of zeros. As the states γ can be expressed as simple functions of the states of (13) and the hysteresis state $W_h(t)$, we know that the solution to the above system is well-posed, and that γ is continuous. Note also that $\bar{\theta}_h(t) \in \Theta_h$, and thus $\bar{\theta}_h$ takes values in a set of finite cardinality; therefore, we can interpret (24) as a switched system, where the switching is governed by the states of the play operators in (5). The stability of such a system can be guaranteed through an LMI condition (Decarlo et al., 2000),

$$(\Sigma_0 + \bar{\theta}_h\bar{B}K_v)^T P + P(\Sigma_0 + \bar{\theta}_h\bar{B}K_v) < 0, \quad \forall \bar{\theta}_h \in \Theta_h$$

where $P > 0$. Such a condition would imply that $V(\gamma) = \gamma^T P \gamma$ is a common Lyapunov function for (24), where $\dot{V} < 0$, $\forall \gamma \neq 0$.

However, since the only element that actually changes is $\bar{\theta}_h$, from the results of Boyd, Ghaoui, Feron, and Balakrishnan (1994) a sufficient condition for the existence of such a P is that

$$(\Sigma_0 + \min(\Theta_h)\bar{B}K_v)^T P + P(\Sigma_0 + \min(\Theta_h)\bar{B}K_v) < 0,$$
$$(\Sigma_0 + \max(\Theta_h)\bar{B}K_v)^T P + P(\Sigma_0 + \max(\Theta_h)\bar{B}K_v) < 0. \qquad (25)$$

Similarly, if a P can be found such that

$$(\Sigma_0 + \min(\Theta_h)\bar{B}K_v)^T P + P(\Sigma_0 + \min(\Theta_h)\bar{B}K_v) + 2\Lambda P < 0,$$
$$(\Sigma_0 + \max(\Theta_h)\bar{B}K_v)^T P + P(\Sigma_0 + \max(\Theta_h)\bar{B}K_v) + 2\Lambda P < 0 \qquad (26)$$

where $\Lambda \in \Re > 0$ then $\dot{V} < -2\Lambda V$, which implies that (24) is exponentially stable, and the tracking error converges to zero with decay rate of at least Λ (Boyd et al., 1994).

Remark 2. One extension of this work would be to consider a modified PI operator (Kuhnen, 2003) for the hysteresis model. This operator adds one-sided deadzones in a superposition to the PI operator so that asymmetric hysteresis nonlinearities can be modeled accurately. The modified PI operator can be fit into our existing framework by extending the definition of $\bar{\theta}_h$, multiplying the result of the current definition with the summation of the weights of the active deadzone operators.

3.1. Specialization to positive real systems

By imposing a positive real assumption on the system, we can arrive at a stronger stability result. Consider the closed-loop system (7)–(9), (11), with

$$v(t) = -K_1 z(t) - K_2 x(t) - K_4 \sigma(t). \qquad (27)$$

Let the system

$$\begin{bmatrix} \dot{\tilde{z}} \\ \dot{\tilde{x}} \end{bmatrix} = \Sigma^* \begin{bmatrix} \tilde{z} \\ \tilde{x} \end{bmatrix} + \mathbb{B}u^*$$
$$\triangleq \begin{bmatrix} F & GC \\ -B(K_1 - \psi) & A_0 - B(K_2 - \lambda) \end{bmatrix} \begin{bmatrix} \tilde{z} \\ \tilde{x} \end{bmatrix} + \begin{bmatrix} 0 \\ Bu^* \end{bmatrix} \qquad (28)$$

$$y = \tilde{\zeta}_1 \triangleq \mathbb{C} \begin{bmatrix} \tilde{z} \\ \tilde{\zeta} \end{bmatrix} \qquad (29)$$

be positive real (Khalil, 2002), where $\tilde{z}$ and $\tilde{x}$ are defined as in (14)–(15), and $u^* \in \Re$ will be defined momentarily. Then, there exists a symmetric positive definite matrix P^* such that

$$P^* \Sigma^* + \Sigma^{*T} P^* = -Q$$
$$P^* \mathbb{B} = \mathbb{C}^T$$

where Q is symmetric and positive definite. This system represents the dynamics portion of our model which has been rendered positive-real by state feedback. This condition is similar to the assumption on the dynamics in Gorbet et al. (2001), where the dynamics of a cascaded controller and a smart material actuator are assumed to be passive. Indeed, for LTI systems, the notions of passivity and positive realness are interchangeable (Kottenstette & Antsaklis, 2010). Note that the controller is not included in this positive real condition. We will now show that under this positive real condition, and with only integral control, the LMI (26) must have a solution.

Let u^* be defined as

$$u^*(t) = \alpha(t) = -K_4 \sigma(t) + \theta_h^T W_h[v; W_h(0)](t) + c_0 y_r$$

where the integrator output σ is governed by

$$\dot{\sigma}(t) = \mathbb{C}[\tilde{z}^T, \tilde{x}^T]^T.$$

Using this definition together with (27) and (28), we notice that we can recover the closed-loop system defined in (23) (excluding the

terms related to η). Let $\tilde{\chi} = [\tilde{z}^T, \tilde{x}^T]^T$ and consider the Lyapunov function candidate

$$V(\tilde{\chi}, \alpha) = \beta \tilde{\chi}^T(t)P^*\tilde{\chi}(t) + 1/2\alpha^2(t) \tag{30}$$

$$= \begin{bmatrix} \tilde{\chi}(t) \\ \alpha(t) \end{bmatrix}^T \begin{bmatrix} \beta P^* & 0 \\ 0 & 1/2 \end{bmatrix} \begin{bmatrix} \tilde{\chi}(t) \\ \alpha(t) \end{bmatrix} \tag{31}$$

where α is defined as in (17). The derivative of V can be written as (using (28)),

$$\begin{aligned}
\dot{V}(\tilde{\chi}, \alpha) &= \beta \tilde{\chi}^T(t)P^*[\Sigma^*\tilde{\chi}(t) + \mathbb{B}\alpha(t)] \\
&\quad + \beta[\Sigma^*\tilde{\chi}(t) + \mathbb{B}\alpha(t)]^T P^*\tilde{\chi}(t) \\
&\quad - \alpha(t)K_4\mathbb{C}\tilde{\chi}(t) + \alpha(t)\theta_h^T \dot{W}_h[v; W_h(0)](t) \\
&= -\beta \tilde{\chi}^T(t)Q\tilde{\chi}(t) + \alpha(t)\tilde{\chi}^T(t)[\beta 2P^*\mathbb{B} - K_4\mathbb{C}^T] \\
&\quad + \alpha(t)\bar{\theta}_h(t)(-K^*\Sigma^*\tilde{\chi}(t) - K^*\mathbb{B}\alpha(t) - K_4\mathbb{C}\tilde{\chi}(t)) \tag{32}
\end{aligned}$$

where $K^* = [K_1, K_2]$. Let β be defined as

$$\beta = K_4/2 \tag{33}$$

and let $\mathbb{F} = -K^*\Sigma^* - K_4\mathbb{C}$. We can then rewrite $\dot{V}$ in the matrix form

$$\dot{V}(\tilde{\chi}, \alpha) = -1/2 \begin{bmatrix} \tilde{\chi}(t) \\ \alpha(t) \end{bmatrix}^T \begin{bmatrix} K_4Q & \bar{\theta}_h(t)\mathbb{F}^T \\ \bar{\theta}_h(t)\mathbb{F} & 2\bar{\theta}_h K^*\mathbb{B} \end{bmatrix} \begin{bmatrix} \tilde{\chi}(t) \\ \alpha(t) \end{bmatrix}. \tag{34}$$

Define $\zeta = [\tilde{\chi}^T, \alpha]^T$, and

$$X = \begin{bmatrix} K_4Q & \bar{\theta}_h(t)\mathbb{F}^T \\ \bar{\theta}_h(t)\mathbb{F} & 2\bar{\theta}_h K^*\mathbb{B} \end{bmatrix}.$$

Let S equal the Schur complement of X, i.e.

$$S = 2\bar{\theta}_h(t)K^*\mathbb{B} - \bar{\theta}_h(t)^2 F[K_4Q]^{-1}F^T. \tag{35}$$

It is well known that X is positive definite if and only if both K_4Q and $S \in \Re$ are positive definite. Assuming that $\bar{\theta}_h > 0$, we can lower bound S with the expression

$$S \geq \left[2K^*\mathbb{B} - \frac{1}{K_4\lambda_{\min}(Q)}\|\theta_h\|_1 F^T F \right] \bar{\theta}_h(t). \tag{36}$$

Note that this equation is independent of the solution to the Lyapunov equation P^*; therefore, if K^* is such that $K^*\mathbb{B} > 0$, we can always find a Q (and therefore a P^*) such that S is positive definite for all $\bar{\theta}_h > 0$. This implies that X is positive definite, and therefore there must exist a sufficiently small Λ such that $X > \Lambda P$, and therefore that P and Λ satisfy the LMI condition (26).

We can now compare our results here with the passivity results achieved in Gorbet et al. (2001) and in similar references such as (Jayawardhana & Andrieu, 2009). In Gorbet et al. (2001), dissipativity (a generalization of passivity) of the Preisach operator is shown between the input and derivative of the output of the operator. In both our results here and the results achieved in Gorbet et al. (2001), by assuming the dynamics are positive real or passive, the properties of the hysteresis operator under consideration allow us to prove stability of the system without any further restrictions on the hysteresis. The principal difference is that because dissipativity can only be shown from the input to the derivative of the output of a hysteresis operator, passivity-based results cannot prove that the tracking error converges to zero, even for constant reference signals. However, our results require that $K^*\mathbb{B} > 0$ and $K_4 > 0$, which may not be satisfied for all positive real systems.

4. Servocompensators for controlling systems with hysteresis

One special stabilizing controller of interest to our work in nanopositioning is the servocompensator (Davison, 1976). This controller is capable of completely canceling disturbances whose internal models are contained in the controller. This property is

also robust to plant uncertainty, as long as the uncertainty does not destabilize the system. The form of this controller is identical to that in (10), where C^* is neutrally stable, with eigenvalues located on the imaginary axis. B^* is chosen to ensure that the pair (C^*, B^*) is controllable. We now assume that the reference signal is generated by a neutrally stable exosystem,

$$\dot{w}(t) = Sw(t) \tag{37}$$

$$y_r(t) = Ew(t). \tag{38}$$

Let us assume that y_r is periodic with period T. We next set up the error coordinate transform,

$$\tilde{z}(t) = z(t) - z^*(t) \tag{39}$$

$$\tilde{x}_1(t) = x_1(t) - y_r(t)$$

$$\vdots$$

$$\tilde{x}_n(t) = x_n(t) - y_r^{(n-1)}(t) \tag{40}$$

where $z^*(t)$ is the steady state solution of

$$\dot{z}^*(t) = Fz^*(t) + Gy_r(t) \tag{41}$$

and the notation $f^{(i)}(t)$ denotes the ith derivative with respect to time. This transform changes the γ dynamics into

$$\begin{aligned}
\dot{\gamma}(t) &= \begin{bmatrix} F & GC & 0 & 0 \\ -B(K_1 - \psi) & A_0 - B(K_2 - \lambda) & -BK_3 & B \\ 0 & B^*C & C^* & 0 \\ 0 & -K_4C & 0 & 0 \end{bmatrix} \gamma(t) \\
&\quad + \begin{bmatrix} 0 \\ -By_r^{(n)}(t) \\ 0 \\ \bar{\theta}_h BK_v \gamma(t) + c_0 y_r^{(1)}(t) \end{bmatrix}. \tag{42}
\end{aligned}$$

Let us assume that we have identified a P such that (26) is satisfied for a given Λ. We can then use $V(\gamma) = \gamma^T P \gamma$ as a Lyapunov function candidate, the derivative of which obeys

$$\dot{V}(\gamma) = -2\Lambda V(\gamma) + 2\gamma^T P[0, -B^T y_r^{(n)}(t), 0, c_0 y_r^{(1)}(t)]^T$$

$$< -2\Lambda \lambda_{\min}(P)\|\gamma\|^2 \tag{43}$$

$$+ 2\lambda_{\max}(P)\|\gamma\| \|[0, -B^T y_r^{(n)}(t), 0, c_0 y_r^{(1)}(t)]\| \tag{44}$$

where $\|\cdot\|$ denotes the Euclidean norm. We can see from this equation that there must exist a sufficiently large γ such that $\dot{V} < 0$; therefore γ enters a bounded positively invariant set and γ remains bounded for all t. However, the disturbance rejection properties of the servocompensator will allow us to draw some further conclusions regarding the performance of the system if we impose a periodicity assumption.

Assumption 1. The steady-state trajectory of $\gamma(t)$ is T-periodic.

Remark 3. The restrictiveness of such an assumption is worth discussing. In Pokrovskii and Brokate (1998), it was shown that if a nonlinear system has an asymptotically stable T-periodic solution, the system still possesses an asymptotically stable T-periodic solution if the system is perturbed by a sufficiently small hysteresis nonlinearity. This result represents the best available theoretical result for showing that a system with hysteresis possesses a T-periodic solution, and this was utilized in Esbrook et al. (in preparation) and Tan and Khalil (2009) to prove stability and periodicity of a system with hysteresis. However, the analysis of Esbrook et al. (in preparation) and Tan and Khalil (2009) requires a sufficiently accurate hysteresis inversion to be incorporated into the control, which we will see in our experimental results may not be ideal. Though theoretical results are lacking, many experimental results reported in the literature have shown that systems with hysteresis seem to poses T-periodic solutions when driven by T-periodic references, regardless of whether inversion is used or not (Bashash & Jalili, 2009; Lee & Salapaka, 2009).

Utilizing Assumption 1, we can now investigate the steady state tracking error, $\tilde{x}_1(t)$. Letting $T = 2\pi/\omega$, we can write $\tilde{x}_1(t)$ in a series form as

$$\tilde{x}_1(t) = \sum_{i=1}^{\infty} R_i \sin(i\omega t + \phi_i). \tag{45}$$

Let us assume that the matrix C^* in our servocompensator (10) has been chosen such that its eigenvalues are located at $\pm jk\omega$, $k \in \rho$, where ρ is a finite-element vector of whole numbers. Because $\tilde{x}_1(t)$ is the input to (10), the servocompensator's error regulation properties will force all components of $\tilde{x}_1(t)$ whose internal models are contained in C^* to have zero amplitude at the steady state. Therefore, $R_i = 0$, $\forall i \in \rho$ in (45).

5. Simulation example: verification of the LMI condition

We now demonstrate the feasibility and effectiveness of our LMI condition with a simulation example. Let us consider a linear system,

$$\mathbb{G}_p(s) = \frac{\omega_n^2}{s^2 + 2\zeta\omega_n s + \omega_n^2} \tag{46}$$

where $\zeta = 0.5$ and $\omega_n = 1$. $\mathbb{G}_p(s)$ is preceded by a PI operator with $\mathbf{r} = [0, r, 2r, 3r]$, with r will be considered as a variable. The weights θ of the operator will be considered a function of r. In particular, for the play operator P_{r_i}, $1 \leq i \leq 3$, θ_i will obey

$$\theta_i(r_i) = \frac{2}{2\mu - 2r_i} \tag{47}$$

where we introduce μ as a design parameter. This choice of θ_i is chosen to make sure the relative gains of the play operators remain constant. By this, we mean that for any $r_i < \mu$, if the input v to $P_{r_i}[v; W_i(0)](t)$ is cycled periodically from $v_{\min} = -\mu$ to $v_{\max} = \mu$, then $\theta_i P_{r_i}[v_{\max}; W_i(0)](t) = 1$. We have illustrated this idea in Fig. 3 for $\mu = 3$. The exception to this rule will be θ_0, which we will fix at one. This cascade of a PI operator and $\mathbb{G}_p(s)$ will be controlled by an integral controller,

$$\dot{\sigma}(t) = y(t) - y_r \tag{48}$$
$$v(t) = -0.25\sigma(t) \tag{49}$$

where $y(t)$ is the output of $\mathbb{G}_p(s)$, and y_r is a constant reference signal. Since our LMI results prove global stability, we will set y_r to be 100. The system described above can be easily fit into the LMI framework (26), with

$$\Sigma_0 + \min(\bar{\theta}_h(r))B^*K_v = \begin{bmatrix} 0 & 1 & 0 \\ -\omega_n^2 & -2\zeta\omega_n & 1 \\ -0.25 & 0 & 0 \end{bmatrix},$$

$$\Sigma_0 + \max(\bar{\theta}_h(r))B^*K_v = \begin{bmatrix} 0 & 1 & 0 \\ -\omega_n^2 & -2\zeta\omega_n & 1 \\ -0.25(1 + \|\theta_h(r)\|_1) & 0 & 0 \end{bmatrix}$$

where $\|\cdot\|_1$ denotes the 1-norm.

To test the viability of our proposed method, we will now begin to increase the value of r until our LMI condition either becomes infeasible or produces a result that cannot guarantee stability. Increasing the value of r makes the hysteresis loops wider, meaning that the control becomes less and less effective at compensating the system. When $r = 0.74$, both LMIs (25) and (26) return results that cannot guarantee stability. We then simulate our system, increasing r each simulation until the tracking error no longer converges to zero. We then denote this value of r as $r_{\max}$. For our setup described here, $r_{\max} = 0.8$, with the system entering a limit cycle rather than converging to zero. Our LMI framework is therefore fairly effective, as it is able to guarantee stability up to 92.5% of $r_{\max}$.

One behavior worth noting is that the value of $r_{\max}$ observed in simulation can vary with the value of y_r. For example, if $y_r = 3$, r can be increased to 0.89 before instability occurs. This would indicate that there is a region of attraction for this system, inside which the tracking error converges to zero. This indicates that the conservatism of our LMI condition is dependent on the value of the reference input y_r.

6. Applications to nanopositioning control

We now confirm the theoretical results of our paper using experiments, in particular those of Section 4. We performed a series of tracking experiments on a commercial nanopositioner (Nano OP-65, from Mad City Labs), and compared the results under different control schemes. Online control implementation and data collection was provided by a dSPACE platform (DS1104). Our work begins with the formulation of the mathematical model of the nanopositioner used to design the controller. A hysteresis operator cascaded with linear dynamics was considered, as illustrated in Fig. 2. Two steps are required to create such a model: first, quasi-static large amplitude signals are used to identify a hysteresis model, then small-amplitude sinusoids are applied over a wide band of frequencies to identify the vibrational dynamics. As the hysteresis of our nanopositioner was not odd-symmetric, we utilized a modified PI operator Γ with 8 play operators and 9 deadzones to model the hysteresis. The weights of the play operators were

$$\theta_h = [0.694, 0.196, 0.041, 0.050, 0.040, 0.050, 0.023, 0.054]$$

and the weights of the deadzones were

$$\theta_d = [1.056, 0.650, 0.327, 0.432, 9.130, -1.138,$$
$$-0.154, -0.787, -0.296].$$

Our vibrational dynamics were modeled by a 4th-order transfer function,

$$\mathbb{G}_p(s) = \frac{4.7 \cdot 10^{17}}{s^4 + 1.6 \cdot 10^4 s^3 + 6.6 \cdot 10^8 s^2 + 5.0 \cdot 10^{12} s + 8.3 \cdot 10^{16}}. \tag{50}$$

In order to improve computation accuracy we used a balanced state-space realization (Zhou, Doyle, & Glover, 1996) of the system (50). This results in the model

$$\dot{x}(t) = 1.0 \times 10^4 \begin{bmatrix} -0.024 & 1.614 & -0.126 & 0.061 \\ -1.614 & -0.266 & 0.721 & -0.161 \\ -0.126 & -0.721 & -1.060 & 1.677 \\ -0.061 & -0.161 & -1.677 & -0.221 \end{bmatrix}$$
$$\times x(t) + \begin{bmatrix} 76.47 \\ 240.4 \\ 242.7 \\ 83.37 \end{bmatrix} u(t)$$

$$y(t) = \begin{bmatrix} 76.47 & -240.4 & 242.7 & -83.37 \end{bmatrix} x(t). \tag{51}$$

Note that, while this nominal dynamics model will be used for controller design, the actual dynamics model of the nanopositioner would have unity gain at DC. This is a consequence of the hysteresis modeling; the gain of the system is effectively incorporated into the hysteresis model. This was discussed in Remark 1. After identifying our modified PI operator, the minimum gain of the hysteresis operator was found to be 4.69, with a maximum of 13.36, while the gain of the plant (51) is 5.62. Let the equation

$$\dot{x}_u(t) = A_u x_u(t) + B_u u(t) \tag{52}$$
$$y_u(t) = C_u x_u(t) \tag{53}$$

denote the canonical form of the dynamics (51) with unity gain, i.e. $y(t) = 5.62 y_u(t)$. We can then fit our nanopositioning system into the form considered in (7)–(9) by letting $m = 0$ and $p = 4$, where

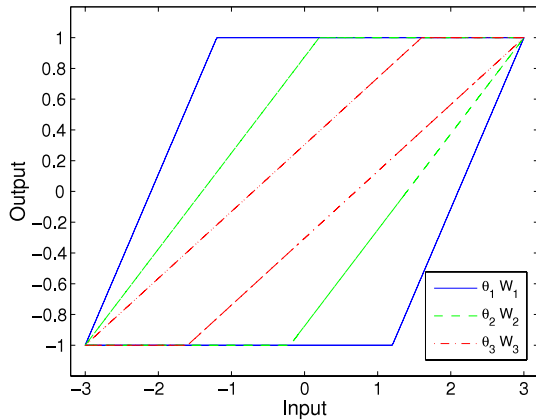$$A_0 + B\lambda = A_u, \quad B = B_u, \quad C = C_u \tag{54}$$

Fig. 3. Hysteresis loops for play operators with equalized relative gains, where r is equal to 0.7, and $\mu = 3$.

Our experiments focused on tracking sinusoidal signals of the form

$$y_r(t) = 20\sin(2\pi\omega t) + 30\,\mu\mathrm{m} \qquad (55)$$

where $\omega = 5, 25, 50, 100, 200$. We utilized two classes of controllers in our tests. First, we utilized the servocompensator controller described in Section 4. A Luenberger observer, based on the model in (51), was implemented to emulate state feedback. Because $u(t)$ is unavailable, the control signal $v(t)$ was used in this observer. The controller gains are chosen using a robust Riccati equation method (Xie & Petersen, 2008) based on the nominal dynamics model (51), a method which was also used in Esbrook et al. (in preparation). Let $v(t) = [K_2, K_3, K_4]\gamma(t)$ denote the control synthesized by this method. Based on the definitions of (54) and Remark 2, $\bar{\theta}_h$ for the modified PI operator considered takes values in the interval $[4.69/5.62, 13.36/5.62] = [0.83, 2.38]$. The boundaries of this interval form the values of $\min(\bar{\theta}_h)$ and $\max(\bar{\theta}_h)$. We can then use the LMI toolbox of MATLAB to solve for the matrix P in (25) or (26).

Four different versions of the servocompensator-based controller are used in our experiments. First, we consider a single-harmonic servocompensator (SHSC) with eigenvalues of $0, \pm j\omega$ and a multi-harmonic servocompensator (MHSC) with eigenvalues of $0, \pm jk\omega$, $k = 1, 2, 3$, both of which are coupled with hysteresis inversion. The inverse of a modified PI operator can be computed in a closed-form, a procedure that is described in Kuhnen (2003). Prior experimental tests have shown the effectiveness of these controllers in nanopositioning control (Esbrook et al., in preparation).

The final two servocompensators used are the SHSC and MHSC designed to operate without hysteresis inversion, the stability of which can be guaranteed by verifying the LMI condition in (26). For example, consider an SHSC with $\omega = 50$. Our controller gains are chosen (according to the method of Esbrook et al., in preparation, and Xie & Petersen, 2008) as

$$[K_2, K_3, K_4]$$
$$= [0.059, 0.081, 0.053, 0.021, -0.002, -1.4, -1.00].$$

The LMI condition (26) can then be verified in the LMI toolbox, with $\Lambda = 4.44$. We also utilize Iterative Learning Control (Wu & Zou, 2007) for comparison purposes in our tests. Like the servocompensator, this method is specialized to periodic signals, and is also robust to plant uncertainty. It is also well accepted in the field of nanopositioning control.

Fig. 4 shows the resulting tracking error of the MHSC and SHSC with and without inversion, together with the Iterative Learning Control (ILC) results. One trend observed in all of the servocompensator-based controllers is that their performance is substantially
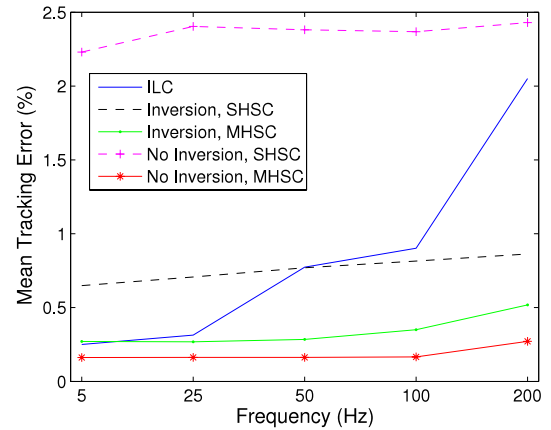

Fig. 4. Mean tracking error for controllers used in experimental trials. SHSC refers to compensation of only the reference harmonic, and MHSC refers to compensation of the first, second, and third harmonics of the reference.
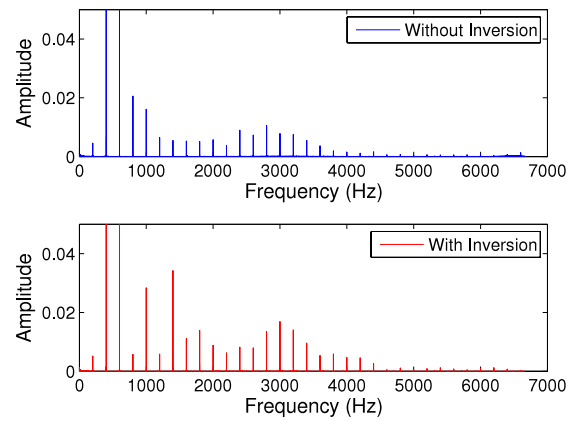

Fig. 5. Frequency spectrum of the tracking error with SHSC with and without inversion. Bump near 3 kHz is caused by the resonance peak of the nanopositioner.

more robust to increasing frequency than ILC. This is particularly true for the servocompensators that do not use inversion, which see very little variation in their performance until the reference reaches 200 Hz. We immediately note that the SHSC without inversion is the worst-performing controller; this is contrasted by the performance of the MHSC without inversion, which is the best-performing controller.

This seeming contradiction can be explained by looking into the frequency spectra of the error signals, provided in Fig. 5. We can see from this graph that the frequency components of the tracking error above 600 Hz are larger when inversion is used as compared to when it is left out. The modified PI operator attempts to approximate the hysteresis with non-smooth play and deadzone operators. Therefore, we expect more high frequency components to be introduced into the system using inversion than when inversion is left out. The performance difference between the controllers is explained by the amplitude of the second and third harmonics, which are much larger without inversion than with inversion. However, once the MHSC is used, these harmonics are compensated and removed from the system, meaning that the overall tracking error is greatly reduced, especially when inversion is not used. In addition, the removal of the hysteresis inversion greatly reduces the computational requirements of the controller. For example, the MHSC without hysteresis inversion averaged a computation time of 28 μs per sampling period, while the MHSC with inversion required 45 μs of computation time. This is a significant savings, especially since the controller possesses half the mean tracking error when the inversion is removed.

7. Conclusions and future work

This paper has provided sufficient conditions for asymptotic or exponential stability of systems with hysteresis. These results contribute to the state of the art due to the lack of restrictions on the order or number of zeros in the dynamics model, and the ability to prove that the tracking error converges to zero when constant references are considered. This framework was also used to prove boundedness under general reference trajectories. Based on these results, we demonstrated the effectiveness of servocompensator-based controllers in nanopositioning systems, where our stability framework allows us to improve the tracking error performance two-fold over existing techniques.

Future work will focus on two directions. First, we will work towards a systematic controller synthesis technique in order to satisfy the LMI conditions (25) and (26). Second, we will attempt to rigorously prove the stability of observer-based controllers in systems with hysteresis by extending our existing framework.

References

Ahrens, J. H., Tan, X., & Khalil, H. K. (2009). Multirate sampled-data output feedback control with application to smart material-actuated systems, 54 (11), 2518–2529.

Barreiro, A., & Banos, A. (2005). Input output stability of systems with backlash. *Automatica*, 1017–1024.

Bashash, S., & Jalili, N. (2009). Robust adaptive control of coupled parallel piezo-flexural nanopositioning stages, 14, 11–20.

Boyd, S., Ghaoui, L. E., Feron, E., & Balakrishnan, V. (1994). *Linear matrix inequalities in system and control theory*. SIAM.

Brokate, M., & Sprekels, J. (1996). *Hysteresis and phase transitions*. New York: Springer-Verlag.

Cavallo, A., Natale, C., Pirozzi, S., & Visone, C. (2003). Effects of hysteresis compensation in feedback control systems, 39 (3), 1389–1392.

Chen, Z., Tan, X., & Shahinpoor, M. (2005). Quasi-static positioning of ionic polymer–metal composite (IPMC) actuators. In *Proceedings of the 2005 IEEE/ASME international conference on advanced intelligent mechatronics* (pp. 60–65).

Croft, D., Shed, G., & Devasia, S. (2001). Creep, hysteresis, and vibration compensation for piezoactuators: atomic force microscopy application. *Journal of Dynamic Systems, Measurement, and Control*, *123*(1), 35–43.

Davino, D., Natale, C., Pirozzi, S., & Visone, C. (2004). Phenomenological dynamic model of a magnetostrictive actuator. *Physica B: Condensed Matter*, *343*(1–4), 112–116.

Davison, E. J. (1976). The robust control of a servomechanism problem for linear time-invariant multivariable systems, 21, 25–34.

Decarlo, R., Branicky, M., Pettersson, S., & Lennartson, B. (2000). Perspectives and results on the stability and stabilizability of hybrid systems, 88 (7), 1069–1082. July.

Devasia, S., Eleftheriou, E., & Moheimani, S. O. R. (2007). A survey of control issues in nanopositioning, 15, 802–823.

Eaton, P., Ragusa, A., Clavel, C., Rojas, C. T., Graham, P., Durán, R. V., & Penadés, S. (2007). Glyconanoparticle–DNA interactions: an atomic force microscopy study, 6 (4), 309–318.

Esbrook, A., Tan, X., & Khalil, H. K. (2012). Control of systems with hysteresis via servocompensation and its application to nanopositioning (in preparation).

Ge, P., & Jouaneh, M. (1996). Tracking control of a piezoceramic actuator, 4 (3), 209–216.

Gorbet, R., Morris, K., & Wang, D. (2001). Passivity-based stability and control of hysteresis in smart actuators, 9 (1), 5–16.

Ikhouane, F., & Rodellar, J. (2007). *Systems with hysteresis: analysis, identification and control using the Bouc–Wen model*. John Wiley & Sons.

Iyer, R., & Tan, X. (2009). Control of hysteretic systems through inverse compensation: inversion algorithms, adaptation, and embedded implementation. *IEEE Control Systems Magazine*, *29*(1), 83–99.

Janaideh, M. A., Rakheja, S., & Su, C.-Y. (2009). A generalized Prandtl–Ishlinskii model for characterizing the hysteresis and saturation nonlinearities of smart actuators. *Smart Materials and Structures*, *18*, 1–9.

Jayawardhana, B., & Andrieu, V. (2009). Sufficient conditions for dissipativity on Duhem hysteresis model. In *Proceedings of the 48th IEEE conference on decision and control* (pp. 4378–4383). December.

Jayawardhana, B., Logemann, H., & Ryan, E. P. (2008). PID control of second-order systems with hysteresis. *International Journal of Control*.

Jayawardhana, B., Logemann, H., & Ryan, E. (2011). The circle criterion and input-to-state stability. *IEEE Control Systems*, *31*(4), 32–67.

Khalil, H. K. (2002). *Nonlinear systems* (3rd ed.). Upper Saddle River, NJ: Prentice Hall.

Kottenstette, N., & Antsaklis, P. J. (2010). Relationships between positive real, passive dissipative, & positive systems. In *Proceedings of the 2010 American control conference* (pp. 409–416).

Kuhnen, K. (2003). Modeling, identification and compensation of complex hysteretic nonlinearities—a modified Prandtl–Ishlinskii approach. *European Journal of Control*, *9*(4), 407–418.

Lee, C., & Salapaka, S. M. (2009). Fast robust nanopositioning: a linear-matrix-inequalities-based optimal control approach, 14 (4), 414–422.

Mayergoyz, I. (1991). *Mathematical models of hysteresis*. New York: Springer-Verlag.

Oh, J., & Bernstein, D. (2005). Semilinear Duhem model for rate-independent and rate-dependent hysteresis, 50 (5), 631–645.

Pokrovskii, A. V., & Brokate, M. (1998). Asymptotically stable oscillations in systems with hysteresis nonlinearities. *Journal of Differential Equations*, *150*, 98–123.

Riccardi, L., Naso, D., Turchiano, B., Janocha, H., & Palagachev, D. K. (2012). PID control of linear systems with an input hysteresis described by Prandtl–Ishlinskii models. In *Proceedings of the 2012 IEEE conference on decision and control* (pp. 5158–5163).

Tan, X., & Baras, J. S. (2005). Adaptive identification and control of hysteresis in smart materials, 50 (6) 827–839.

Tan, X., & Khalil, H. K. (2009). Two-time-scale averaging of systems involving operators and its application to adaptive control of hysteretic systems. In *Proceedings of the 2009 American control conference* (pp. 4476–4481).

Tao, G., & Kokotovic, P. V. (1995). Adaptive control of plants with unknown hystereses, 40 (2), 200–212.

Tarbouriech, S., Prieur, C., & Queinnec, I. (2010). Stability analysis for linear systems with input backlash through sufficient LMI conditions. *Automatica*, 1911–1915.

Valadkhan, S., Morris, K., & Khajepour, A. (2010). Stability and robust position control of hysteretic systems. *International Journal of Robust and Nonlinear Control*, *20*(4), 460–471.

Visintin, A. (1994). *Differential models of hysteresis*. New York: Springer-Verlag.

Webb, G. V., Lagoudas, D. C., & Kurdila, A. J. (1998). Hysteresis modeling of sma actuators for control applications. *Journal of Intelligent Material Systems and Structures*, *9*(6), 432–448.

Wu, Y., & Zou, Q. (2007). Iterative control approach to compensate for both the hysteresis and the dynamics effects of piezo actuators, 15 (5), 936–944.

Xie, L., & Petersen, I. (2008). Perfect regulation with cheap control for uncertain linear systems: a Riccati equation approach. *IET Control Theory and Applications*, *2*, 782–794.

Zhong, J., & Yao, B. (2008). Adaptive robust precision motion control of a piezoelectric positioning stage, 16, 1039–1046.

Zhou, K., Doyle, J. C., & Glover, K. (1996). *Robust and optimal control* (3rd ed.). Upper Saddle River, NJ: Prentice Hall.

Alex Esbrook received the B.S. and Ph.D. degrees in electrical engineering from Michigan State University, East Lansing MI, USA, in 2008. From May of 2008 to December of 2012, he was a member of the Smart Microsystems Laboratory in the Department of Electrical and Computer Engineering at Michigan State University. His research interests include control of systems with hysteresis, regulation theory, adaptive systems and automotive control. Dr. Esbrook received an award for best session presentation at the 2010 American Control Conference, and an honorable mention for the 2009 National Science Foundation graduate research fellowship.

Xiaobo Tan received the B.Eng. and M.Eng. degrees in automatic control from Tsinghua University, Beijing, China, in 1995 and 1998, respectively, and the Ph.D. degree in electrical and computer engineering from the University of Maryland, College Park, in 2002.

From September 2002 to July 2004, he was a Research Associate with the Institute for Systems Research at the University of Maryland. He joined the faculty of the Department of Electrical and Computer Engineering at Michigan State University (MSU) in 2004, where he is currently an Associate Professor. His current research interests include modeling and control of smart materials, electroactive polymer sensors and actuators, biomimetic robotic fish, mobile sensing in aquatic environments, and collaborative control of autonomous systems.

Dr. Tan is an Associate Editor of Automatica and a Technical Editor of IEEE/ASME Transactions on Mechatronics. He served as the Program Chair for the 15th International Conference on Advanced Robotics (ICAR 2011). He was a guest editor of IEEE Control Systems Magazine for its February 2009 issue's Special Section on Modeling and Control of Hysteresis. Dr. Tan received the NSF CAREER Award in 2006, the 2008 ASME DSCD Best Mechatronics Paper Award (with Yang Fang) in 2009, and the Teacher-Scholar Award from MSU in 2010.

Hassan K. Khalil received the B.S. and M.S. degrees in electrical engineering from Cairo University, Egypt, in 1973 and 1975, respectively, and the Ph.D. degree from the University of Illinois, Urbana–Champaign, in 1978, all in electrical engineering.

Since 1978, he has been with Michigan State University (MSU), where he is currently University Distinguished Professor of Electrical and Computer Engineering. He has consulted for General Motors and Delco Products, and published several papers on singular perturbation methods and nonlinear control. He is the author of *Nonlinear Systems* (Macmillan 1992; Prentice Hall 1996 & 2002) and coauthor of *Singular Perturbation Methods in Control: Analysis and Design* (Academic Press 1986; SIAM 1999).

Dr. Khalil was named IEEE Fellow in 1989 and IFAC Fellow in 2007. He received the 1989 IEEE-CSS George S. Axelby Outstanding Paper Award, the 2000 AACC Ragazzini Education Award, the 2002 IFAC Control Engineering Textbook Prize, the 2004 AACC O. Hugo Schuck Best Paper Award, and the 2009 AGEP Faculty Mentor of the Year Award. At MSU he received the 2003 Teacher Scholar Award, the 1994 Withrow Distinguished Scholar Award, and the 1995 Distinguished Faculty Award. He served as Associate Editor of the IEEE TRANSACTIONS ON AUTOMATIC CONTROL, *Automatica*, and *Neural Networks*, and as Editor of *Automatica* for nonlinear systems and control. He was Registration Chair of the 1984 CDC, Finance Chair of the 1987 ACC, Program Chair of the 1988 ACC, and General Chair of the 1994 ACC.